AIAA Journal, Available online 18 November 2024
DOI:10.2514/1.j064595

Coupled Fan-Intake Dynamic Distortion Characterization at Crosswind Conditions

Tommaso Piovesan,[*] Pavlos K Zachos,[†] and David G MacManus[‡]
Faculty of Engineering and Applied Sciences, Cranfield University, UK

Kushal Kempaiah[§] and Dirk Michaelis[**]
LaVision GmbH, Göttingen, Germany

Bart van Rooijen [††]
German-Dutch Wind Tunnels, Marknesse, The Netherlands

Mehdi Vahdati [‡‡]
Faculty of Engineering, Imperial College London, UK

and

Christopher Sheaf [§§]
Rolls-Royce plc., Derby, UK

I. Introduction

The operation and aerodynamics of an aeroengine under crosswind conditions is dominated by complex unsteady interactions between the fan, the intake, and the ground plane. This can potentially influence the aerodynamic and mechanical engine-intake compatibility and for this reason knowledge of these complex flow field characteristics is required. [1]. The intake aerodynamics are primarily characterized by the formation of a ground vortex, due to the

[*] Doctoral Researcher, Centre for Propulsion and Thermal Power Engineering.
[†] Reader in Propulsion Aerodynamics, Centre for Propulsion and Thermal Power Engineering, AIAA Senior Member. *Corresponding author, p.zachos@cranfield.ac.uk*
[‡] Professor in Propulsion Aerodynamics, Centre for Propulsion and Thermal Power Engineering, AIAA Member.
[§] Researcher.
[**] Product Manager for Flow Measurement.
[††] Project Manager.
[‡‡] Professor in Thermo-Fluids, Department of Mechanical Engineering.
[§§] Installations Aerodynamics Specialist, Cold End Centre of Excellence.

interaction between the ingested mass flow and the ground, as well as significant lip flow separation, which is linked to total pressure and swirl distortions at the fan face.

The flow physics of ground vortex formation and behavior is a complex problem with several previously studies focused on understanding the flow mechanisms. Siervi et al. [2] conducted an experimental and analytical investigation to determine the key mechanisms of the inlet-vortex formation. This study identified the ratio of the intake to crosswind velocity as an important parameter that determines onset of the ground vortex for a given ground clearance. An increase in aero-engine bypass ratio typically leads to a reduction in the ground clearance which results in a wider range of operating conditions for which a ground vortex forms and affects the intake aerodynamics. In addition, there is an interest in the development of shorter intakes for ultra-high bypass ratio configurations to reduce cruise fuel burn. For these intakes, the crosswind performance, ground vortex characteristics, and interaction between the intake and the fan are key design and operational considerations.

With the development of new experimental techniques able to provide high spatial resolution data, significant contributions were made initially by Murphy [1], Wang and Gursul [3], Übelacker et al. [4], and more recently by Courtine et al. [5]. These works used non-intrusive, optical methods to partially characterize the aerodynamics for intakes at various off design conditions, including crosswind. A notable recent advancement in intake flow characterization methods was reported by Kempaiah et al. [6] who demonstrated the synchronous measurement of the three-velocity components across a notional fan face for an aspirated intake (i.e. no fan rotor in the intake) under crosswind and incidence conditions in an industrial wind tunnel setting, which was never shown before. Kempaiah's study enabled the unsteady characterization of pertinent flow topologies such as the ground vortex and the windward separation, the stability limits of the investigated intakes as well as the dynamic distortion signatures across the operating regimes with data resolution at least two orders of magnitude in relation to intrusive techniques. The importance of validating current numerical capabilities for intakes under crosswind was recently acknowledged by the AIAA 5th Propulsion Aerodynamics Workshop which dedicated a coordinated effort to validate modern numerical tools using previous experimental results for a pertinent test case [7]. However, in the majority of previous studies, only aspirated intakes were investigated, where the influence of the fan rotor on the inlet flow characteristics and the ground vortex formation was not accounted for, although its importance was fully acknowledged [8] [9]. An effort to address this gap was recently presented by Stuermer and Geisler [10] who used low-bandwidth PIV to measure fan

face swirl during a full-scale engine crosswind test. However, the complexity of the experimental setup and engine configuration yielded an only partially successful experiment with very limited data to support conclusive outcomes.

Following the optical experiments at an aspirated intake reported by Kempaiah [6], the current paper shows optical, unsteady velocity and swirl distortion measurements within a coupled fan-intake configuration (i.e. with a fan rotor in place). The herein presented test campaign delivered fan-face unsteady velocity and swirl distortion measurements across a range of crosswind speeds and fan operating points at a spatial resolution at least two orders of magnitude greater than conventional distortion characterisation methods. The experiments were conducted within an industrial environment, which highlights the maturity of such methods to potentially become part of standard industrial practice.

This technical note describes the experimental setup and demonstrates the viability of S-PIV to measure fan face velocity and swirl flow distortion for a coupled intake-fan configuration. This has never been previously demonstrated for such a configuration and is the core novel contribution of this work. These initial findings indicate that such high-resolution measurements have the potential to fundamentally improve the understanding of the complex aerodynamic interactions between fans and intakes under crosswind conditions and will potentially enable the development of future closely coupled propulsion systems.

II.Summary of Experimental Setups

The experiments were conducted at DNW's Large Low-speed Facility (DNW-LLF) configured as an open jet with a working section cross-section of 6x6 m^2. A view of the installed test article is shown in Figure 1 where the lamppost support system and the ground plane are also indicated. The test article included the intake of a generic high bypass ratio civil turbofan aero engine. The aero-line definition of the intake was the sideline of the through flow nacelle from the NASA Common Research Model (CRM), which was previously documented by Vassberg et al. [11]. The model had an axisymmetric intake with no droop or scarf and with a length to highlight diameter ratio L/D_h = 0.425, which is slightly higher than proposed intake designs for novel, very high bypass ratio engines [12]. The intake was a scaled model of a full-scale aero-engine and had a highlight diameter of 275 mm. The selected scaling factor was dictated by the fan rotor diameter of the already available turbine power simulator (TPS) unit at DNW. Standard industrial practice was applied to ensure that no interference between the wind tunnel's free jet and the test article was present. The intake boundary layer was tripped upstream of the highlight plane on the outer fan cowl surface, to ensure a fully turbulent boundary layer entering the intake. The model was powered by a turbine power simulator (TPS) unit that

comprised a single stage fan with a diameter of 260 mm (10.2") at the fan face. The fan had 19 rotor and 25 stator blades and an elliptical spinner (Figure 2). The baseline aerodynamic design and performance characteristics of the fan were previously described by Schnell et al. [13]. Externally supplied compressed air was used to power a turbine which drives the fan and induces air flow into the model. This air supply was fed into the model via an inlet duct housed within the support pylon indicated as pressure inlet in Figure 2. The operating point of the fan during the experiments was determined via a rake system installed at the bypass and core exhaust ducts which was able to measure both total temperature and pressure around the annulus. The fan pressure ratio was calculated as the ratio of the time averaged, area averaged total pressure at the exit of the fan over the freestream tunnel total pressure. The total pressure and temperature as well as the static pressure at the exit of the fan were used to calculate the ideal Mach number and velocity at the fan exit nozzle. The corrected fan flow was determined through a discharge coefficient that was established during the fan calibration pre-tests. A similar approach was used to calculate the corrected flow through the TPS core. For the crosswind tests, a ground plane was used (Figure 1) with a size of approximately 2x2 m^2. The non-dimensional ground clearance was h/D_h=0.3, which is a representative value for modern under-wing engine installations. The ground plane boundary layer was tripped to ensure turbulent flow. The boundary layer profile was measured at a reference position on the ground plane upstream of the intake. For both cases reported herein, ground plane boundary layer had a thickness $\delta \approx 14.5\ mm$ and a shape factor $H \approx 1.2$ suggesting a fully turbulent boundary layer.

The primary goal of the experiment was to demonstrate the industrial application of non-intrusive, crossflow distortion measurements within a representative turbofan intake coupled with a fan rotor. To enable the optical measurements, the intake model included two transparent rings that allowed laser illumination of 2 crossflow planes ahead of the fan face. PIV Planes 1 (P1) and 2 (P2) centers were located 40 mm and 30 mm upstream of the fan face, respectively (Figure 2). The measurement plane illumination was provided by x2 Quantel Evergreen dual-pulsed Nd:YAG lasers were used (532 nm, 2x200mJ at 15 Hz) which were located underneath the ground plane. A set of optics converted the laser beams into light sheets which were delivered to the P1 and P2 locations within the intake through an acrylic window in the ground plane from the lower left and lower right side, respectively. A similar setup was previously used by Kempaiah et al. during the previous aspirated intake tests [6]. This dual laser setup was required to mitigate the shadow zones generated by the fan spinner (Figure 2). The two lasers were installed on a linear traverse that allowed the light sheets to be translated parallel to the engine axis to enable illumination of the P1

and P2 planes (Figure 2). The light sheets were independently aligned within the optical ring of the model and subsequently fine-tuned to optimize the axial overlap. The seeding flow was atomized particles of Di-Ethyl-Hexyl Sebacate (DEHS) which were injected into the tunnel's main air stream via a 2 m by 2 m seeding rake installed in the settling chamber. The exact axial location and seeding density were remotely control and optimized during the experiment. For image recording, a multi-camera variable geometry PIV system was used. The multi-camera system was previously described by Kempaiah et al. [6] as part of aspirated intake tests. The system comprised 6-off LaVision Imager sCMOS cameras (2,560 x 2,160 px, 16 bits, 6.5 μm pixel size). Each camera was installed on a rotation unit with remote control to adjust the planar Scheimpflug angle and focus settings. Four of the cameras were equipped with an additional remote control of a second Scheimpflug axis. The cameras had 300 mm focal length lens to enable imaging from a long stand-off distance. The camera lines of sight were defined in such a way that each part of the measurement plane was imaged by at least two cameras to enable stereoscopic PIV measurements. The six-camera array was installed on a frame which was mounted on an elevated platform located outside of the flow stream, at the starboard side of the test section approximately at the same height as the model. The stand-off distance between the camera array and the measurement plane was between 7 and 8 m. The PIV data were processed using LaVision's DaVis 11.0 software. All PIV measurements were conducted in a phase-locked arrangement to account for the fan rotational speed. Consequently, the fan blades were imaged at an approximately fixed azimuthal location across the entire dataset. This helped with the background image subtraction as part of the post-processing method and improved the signal to noise ratio of the PIV data. The optical setup and image post-processing yielded a final PIV spatial resolution of approximately 1.5 mm^2 across the measurement plane for all investigated cases. This corresponds to total of approximately 18,000 synchronous three-component velocity vectors at the measurement planes, acquired at a temporal frequency of 15 Hz. Each PIV data set comprised 1,000 snapshots, which were used to produce the flow statistics.

III. Initial Results

The test conditions ranged between 0 and 30 knots crosswind speeds with TPS rotational speeds between 13,500 and 28,500 RPM in typical steps of approximately 1,500 RPM. These corresponded to ISA-normalized fan flow rates across a range between 4 – 8.3 kg/s and pressure ratios between 1.06 to 1.28. The highest fan rotational speed corresponds to a a relative to rotor Mach number of 1.05. The PIV velocity fields occupy the measurement plane up

to about 96% of its radius. Excessive laser light reflections near the wall penalized the signal to noise ratio and yielded only spurious vectors in this area which were discarded during the image processing.

Instantaneous, normalized, out-of-plane velocity and swirl angle distributions for two cases with Mass Flow Capture Ratio ($MFCR = \dot{m}/\rho_\infty V_\infty A_{hi}$) of 17.5 and 8.9 are shown in Figure 3. For the MFCR definition, $\dot{m}$ denotes the intake's mass flow rate, ρ_∞ the free stream density, V_∞ the free stream flow velocity, and A_{hi} the intake's highlight area. At both shown conditions, the intake's Reynolds number based on its highlight diameter ($Re = \rho_\infty V_\infty D_{hi}/\mu$, μ denoting the dynamic viscosity at free stream conditions) was $4.2 \bullet 10^5$. This is lower than a real flight condition, suggesting a potentially different separation onset between sub- and full-scale conditions [14] [15] [16]. However, for the crosswind condition, the underpinning mechanisms of the intake swirl distortion would be scale (and hence Reynolds) independent, despite their scale-dependent onset. For MFCR=17.5, the flow at the inner surface of the intake was attached, with the main swirl distortion associated with the ingested ground vortex core also clearly captured at the lower part of the plane. This is evident in the sample snapshots of normalized axial velocity (Figure 3a) and swirl angle (Figure 3c). The PIV resolution was sufficient to capture the ground vortex core with approximately 30 velocity vectors identified in the general vortex area and about 12 vectors along a line of the vortex core between maximum and minimum circumferential velocity. For a lower fan speed (13.5 krpm) at fixed crosswind velocity of 12.5 knots and MFCR of 8.9, there is a diffusion induced flow separation at the windward inner side of the intake. The signature of the ground vortex is still evident in the axial velocity and swirl angle distributions in lower part of the plane (Figure 3b and d). The PIV successfully captured the extensive instantaneous lip separation with areas of reverse flow, notable changes in swirl angle as well as the local increases in axial velocity (Figure 3b and d).

The instantaneous velocity snapshots were used to compute the time averaged velocity and swirl angle distributions for the two cases (Figure 4). The 1,000 samples were sufficient to produce representative statistics as the standard deviation of the swirl angle varied by less than 1% after approximately 700 samples for both cases. The in-plane velocity vectors are shown on the contour for visualization purposes. The measured flow topologies are broadly aligned with previous measurements at similar operating conditions acquired at the notional fan face within an aspirated intake [6]. For example, the ground vortex position is similar as well as the extent of the separation on the windward lip. Based on previous computational studies, it is expected that the fan rotor would have an influence on the intake's distortion characteristics possibly by improving the flow separation bounds and reducing the levels of

inlet flow distortion [8] [9]. However, the presented test case does not allow for quantification of the effect of the rotor as the directly comparable data for an aspirated configuration is not available.

The time average swirl angle distributions indicate a maximum absolute swirl angle of approximately 30° around the ground vortex and separation regions (Figure 4c and d). For this test arrangement, where the fan rotation is in the anti-clockwise direction, this is considered as a co-rotating ground vortex. In the tip region, for the time-averaged data, the swirl from the ground vortex and the separation is predominately in the counter-clockwise direction and will result in negative incidence on the rotor. At a lower blade span, the main effect is due to the inner part of the ground vortex, where there are locally large swirl angles with positive incidence to the rotor for both the attached (MFCR=17.5) and separated (MFCR=8.9) cases. In addition, the ground vortex and separated flow regions are also associated with high levels of unsteadiness. For example, the standard deviation of the swirl angle was over 30° in the ground vortex core region and the separated region for MFCR=8.9 (Figure 5). This suggests that instantaneous, peak swirl distortion events with very high values, and variations, of incidence should be expected locally.

IV. Conclusions and Future Prospects

For both shown cases, PIV measurements captured the key flow features including the windward flow separation and the ground vortex. Similar results with high quality optical data were achieved across the range of operating conditions, including cases at higher fan operating points. Current work in progress is linked to post-processing the PIV datasets across the entire test matrix.

Overall, this work has demonstrated for the first time the ability to acquire 3-component PIV measurements of fan-face flow distortions at a podded intake-fan configuration within an industrial environment. Several innovations were put in place over the course of the programme. These innovations include bespoke design of the test article and ground plane to enable laser access, design, setup, and remote operation of the multi-camera PIV system as well as the post-processing of the optical data to almost nullify the background reflections caused to PIV images by the rotor blades. The work delivers significant advancements of current capability in characterizing fan face distorted flows, that will eventually impact the design and development of future, closely integrated propulsion systems.

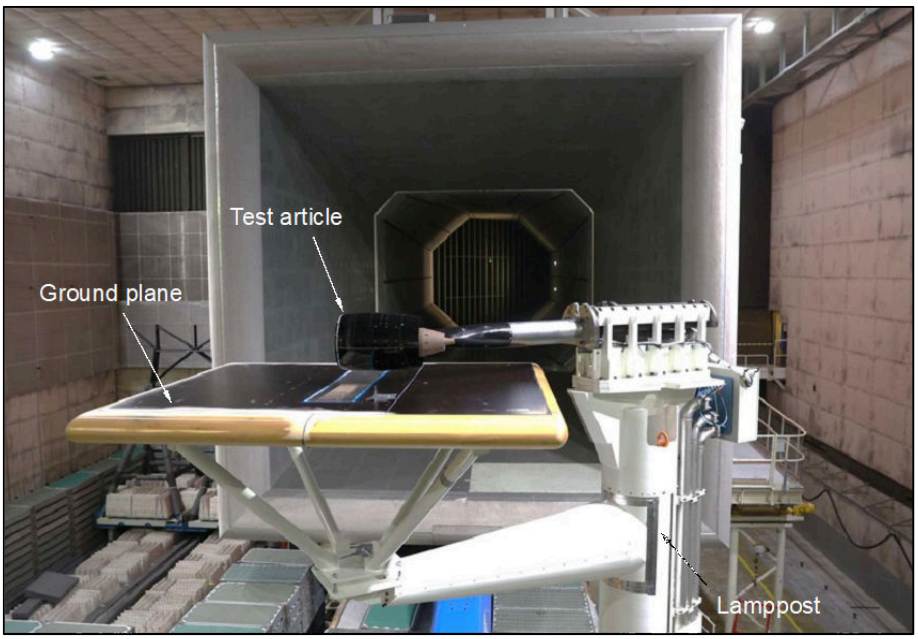

Figure 1 Test article and ground plane installed at DNW-LLF open working section via a lamppost system (view parallel to crosswind direction, looking downstream).

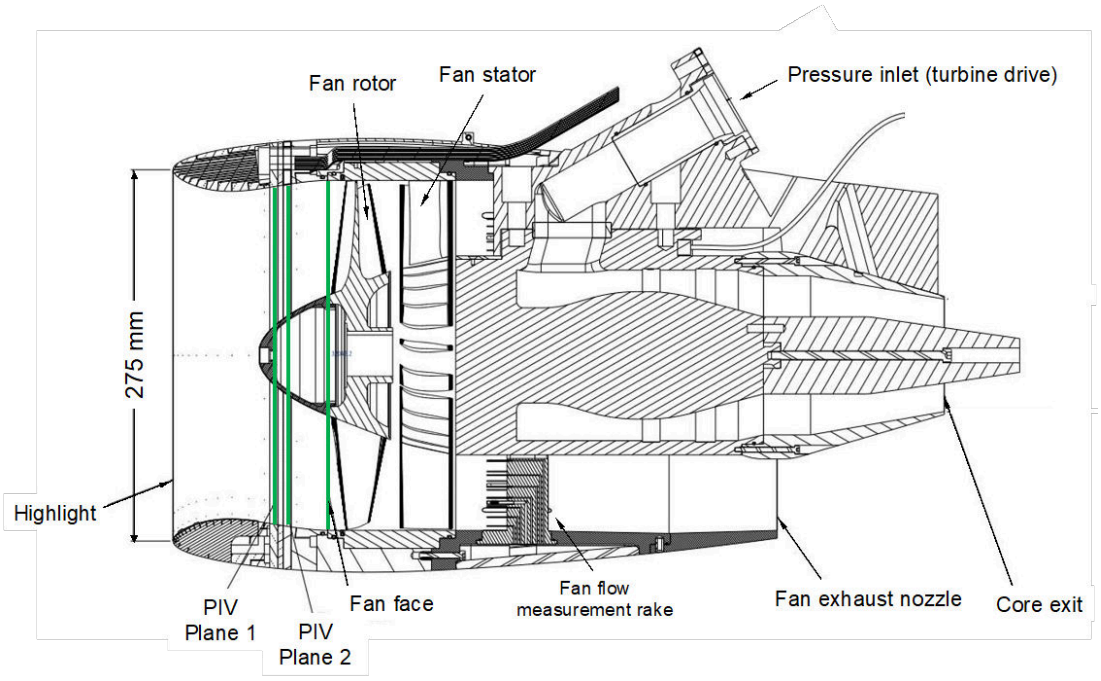

Figure 2 Test article schematic indicating fan face and PIV measurement planes.

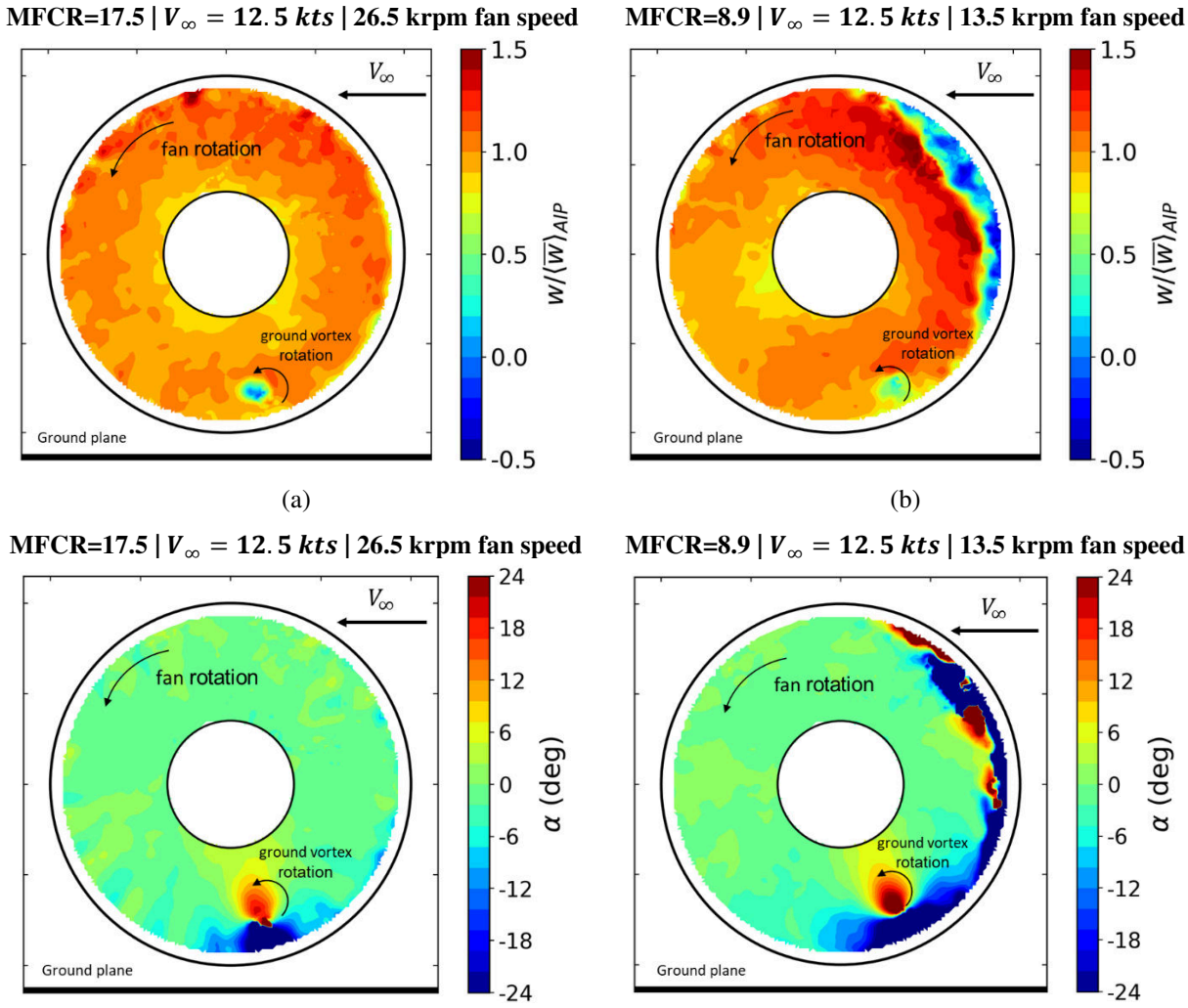

Figure 3 Instantaneous, normalized out-of-plane velocity and swirl angle distributions across PIV Plane 1. View looking downstream.

MFCR=17.5 | $V_\infty = 12.5\ kts$ | 26.5 krpm fan speed

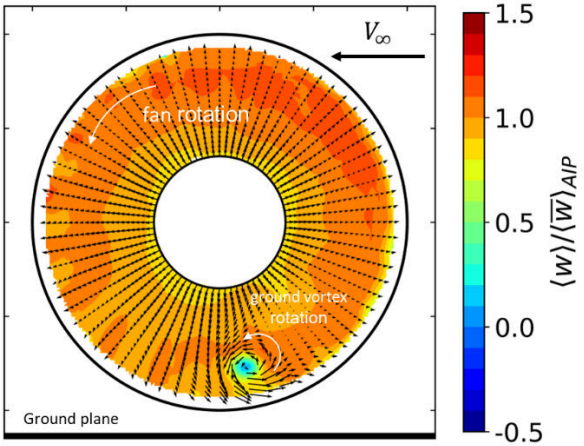

(a)

MFCR=8.9 | $V_\infty = 12.5\ kts$ | 13.5 krpm fan speed

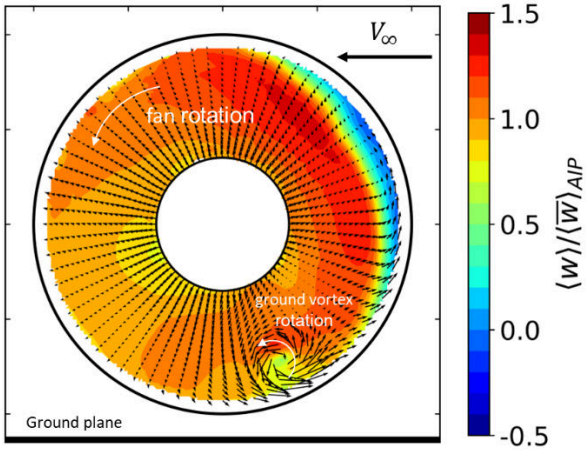

(b)

MFCR=17.5 | $V_\infty = 12.5\ kts$ | 26.5 krpm fan speed

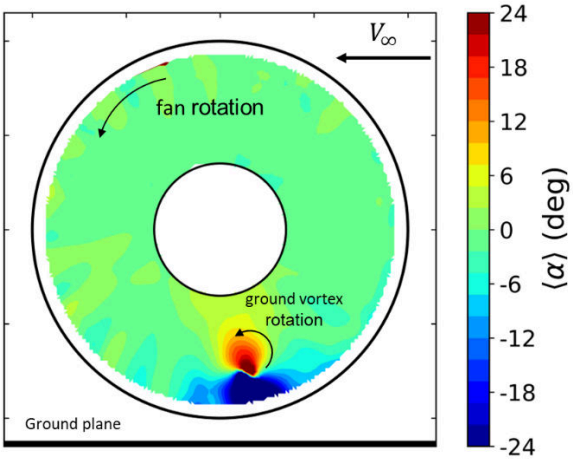

(c)

MFCR=8.9 | $V_\infty = 12.5\ kts$ | 13.5 krpm fan speed

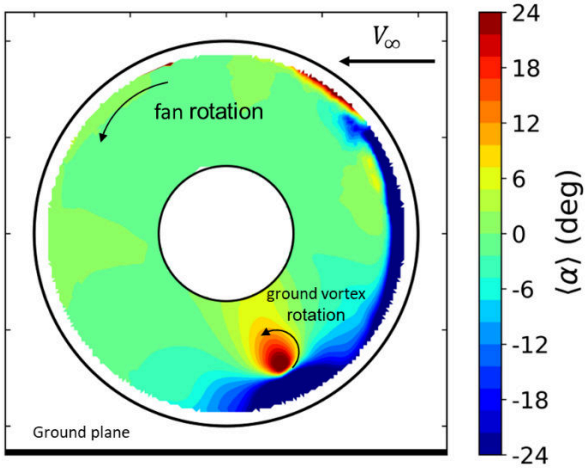

(d)

Figure 4 Time-averaged, normalized, out-of-plane velocity and swirl angle distributions across PIV Plane 1. View looking downstream.

MFCR=17.5 | $V_\infty = 12.5\ kts$ | 26.5 krpm fan speed

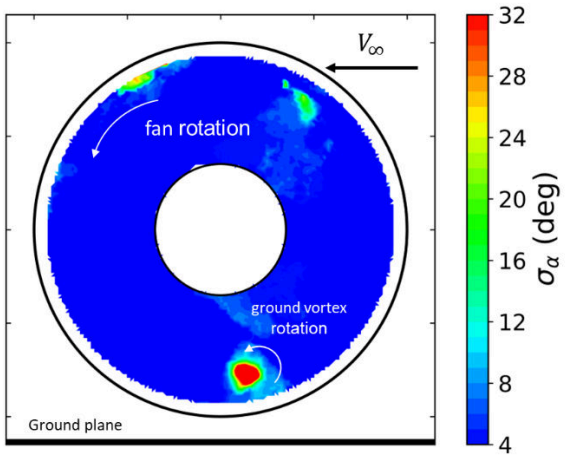

(a)

MFCR=8.9 | $V_\infty = 12.5\ kts$ | 13.5 krpm fan speed

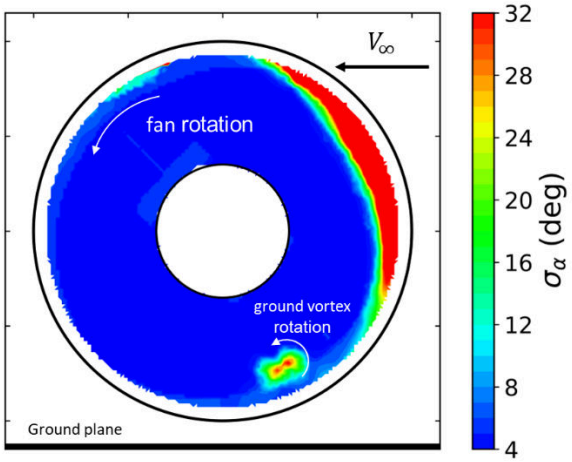

(b)

Figure 5 Standard deviation of the swirl angle across PIV Plane 1. View looking downstream.

Funding Sources

This project has received funding from the Clean Sky 2 Joint Undertaking (JU) under grant agreement No 864911. The JU receives support from the European Union's Horizon 2020 research and innovation programme and the Clean Sky 2 JU members other than the Union. The authors remain grateful to Prof Nick Cumpsty of Imperial College London for the support and insights over the duration of the work.

References

[1] Murphy, J. P., MacManus, D. G., and Sheaf, C. T., "Experimental Investigation of Intake Ground Vortices During Takeoff," *AIAA Journal*, Vol. 48, No. 3, 2012, pp. 688–701. https://doi.org/10.2514/1.45896

[2] Siervi, F. D., Viguier, H. C., Greitzer, E. M., and Tan, C. S., "Mechanisms of Inlet-Vortex Formation," *Journal of Fluid Mechanics*, Vol. 124, No. 1, 1982, p. 173. https://doi.org/10.1017/s0022112082002456

[3] Wang, Z., and Gursul, I., "Unsteady Characteristics of Inlet Vortices," *Experiments in Fluids*, Vol. 53, No. 4, 2012, pp. 1015–1032. https://doi.org/10.1007/s00348-012-1340-2

[4] Übelacker, S., Hain, R., and Kähler, C. J., "Experimental Investigation of the Flow in a Stalling Engine Inlet," *32nd AIAA Applied Aerodynamics Conference*, 2014. https://doi.org/10.2514/6.2014-2839

[5] Courtine, S., Bouchet, J.-P., Guibert, A., Gauducheau, B., Costa, R. M. e, and Raynal, S., "Experimental Characterization of Intake Ground Vortex Ingestion under Crosswind Conditions in Wind Tunnel," *56th 3AF International Conference on Applied Aerodynamics*, 2022.

[6] Kempaiah, K. U., Piovesan, T., Zachos, P. K., Michaelis, D., Gebbink, R., Rooijen, B. van, Prieto, D. G., MacManus, D., Sciacchitano, A., and Sheaf, C., "High-Resolution Turbofan Intake Flow Characterization by Automated Stereoscopic-PIV in an Industrial Wind Tunnel Environment," *Measurement Science and Technology*, Vol. 35, No. 2, 2024, p. 025210. https://doi.org/10.1088/1361-6501/ad0ea0

[7] Babcock, D. A., Neto, L. T., Davis, Z., Karman-Shoemake, K., Woeber, C., Bajimaya, R., and MacManus, D., "Summary of the 5th Propulsion Aerodynamics Workshop: Inlet Cross-Flow Results," *AIAA SCITECH 2022 Forum*, 2022. https://doi.org/10.2514/6.2022-0814

[8] Mohankumar, B., Hall, C. A., and Wilson, M. J., "Fan Aerodynamics with a Short Intake at High Angle of Attack," *Journal of Turbomachinery*, Vol. 143, No. 5, 2021. https://doi.org/10.1115/1.4050606

[9] MacManus, D. G., and Slaby, M., "Intake Ground Vortex and Computational Modelling of Foreign Object Ingestion," *The Aeronautical Journal*, Vol. 119, No. 1219, 2015, pp. 1123–1145. https://doi.org/10.1017/s0001924000011167

[10] Stuermer, A. W., and Geisler, R., "CFD Modeling of Turbofan Intake Aerodynamics at Crosswind Conditions," *AIAA AVIATION 2023 Forum*, 2023. https://doi.org/10.2514/6.2023-3306

[11] Vassberg, J., Dehaan, M., Rivers, M., and Wahls, R., "Development of a Common Research Model for Applied CFD Validation Studies," AIAA 2008-6919, *26th AIAA Applied Aerodynamics Conference*, 2008. https://doi.org/10.2514/6.2008-6919.

[12] Peters, A., Spakovszky, Z. S., Lord, W. K., and Rose, B., "Ultrashort Nacelles for Low Fan Pressure Ratio Propulsors," *Journal of Turbomachinery*, Vol. 137, No. 2, 2015, p. 021001. https://doi.org/10.1115/1.4028235

[13] Schnell, R., Goldhahn, E., and Julian, M., "Design and Performance of a Low Fan-Pressure-Ratio Propulsion System," *Proceedings of the 24th International Symposium on Air Breathing Engines 2019 (ISABE 2019)*, Canberra, Australia, 2019.

[14] Motycka, D. L., "Reynolds Number and Fan/Inlet Coupling Effects on Subsonic Transport Inlet Distortion," *Journal of Propulsion and Power*, Vol. 1, No. 3, 2012, pp. 229–234. https://doi.org/10.2514/3.22785.

[15] Hall, C. A., and Hynes, T. P., "Measurements of Intake Separation Hysteresis in a Model Fan and Nacelle Rig," *Journal of Propulsion and Power*, Vol. 22, No. 4, 2012, pp. 872–879. https://doi.org/10.2514/1.18644

[16] Younghans, J., Hoelmer, W., and Stockman, N., "Low Speed Effects of Reynolds Number and Lip Geometry on High Bypass ratio Inlet Performance," AIAA-82-0059, *20th Aerospace Sciences Meeting*, 1982. https://doi.org/10.2514/6.1982-59

Coupled fan-intake dynamic distortion characterization at crosswind conditions

Piovesan, Tommaso

2025-02

Piovesan T, Zachos PK, MacManus DG, et al., (2025) Coupled fan-intake dynamic distortion characterization at crosswind conditions. AIAA Journal, Volume 63, Issue 2, February 2025, pp. 811-815
https://doi.org/10.2514/1.j064595